The supplementary material and Supporting information

Anti-androgenic potential of the fruit extracts of certain Egyptian *Sabal* species and their genetic variability studies; A metabolomic-molecular modeling approaches

Supporting information

Table S1: Primer Name, sequences, number of total bands, polymorphic bands, percentage of polymorphism of SCoT primers.

Table S2: Genetic similarities between the four *Sabal* species based on Jaccard's similarity coefficient of SCoT data.

Table.S3. Primer Name, sequences, number of total bands, polymorphic bands, percentage of polymorphism of CBDP primers.

Table S4: Genetic similarities between the four *Sabal* species based on Jaccard's similarity coefficient of CBDP data.

Table S5: The Reduction% in weights of sex organs of male Sprague Dawley rats after administration of the fruit methanolic extracts of *S. blackburniana, S, causiarum and S. palmetto.*

Fig S1. Total ion chromatogram of *S. blackburniana* fruits (negative ionization mode).

Fig S2. Total ion chromatogram of *S. yapa* fruits (negative ionization mode).

Fig S3. Total ion chromatogram of *S. palmetto* fruits (negative ionization mode).

Fig S4. Total ion chromatogram of S. causiarum fruits (positive ionization mode).

Fig.S5. Putative compounds annotated from the methanolic extract of the selected *Sabal* species. Orange-colored compounds showed docking scores <-7 kca/mol against 5-α-reductase 2, but got high ΔG binding value (>-7kcal/mol).

Fig.S6. Putative compounds (1-30) annotated from the methanolic extract of the selected *Sabal* species. Orange-colored compounds showed docking scores <-7 kca/mol against 5-α-reductase 2, but got high ΔG binding value (>-7kcal/mol). Green-colored compounds got docking score and ΔG binding value <-7 kcal/mol.

Fig.S7. Putative compounds annotated from the methanolic extract of the selected *Sabal* species. Orange-colored compounds showed docking scores <-7 kca/mol against 5-α-reductase 2, but got high ΔG binding value (>-7kcal/mol).

Fig.S8. Putative compounds annotated from the methanolic extract of the selected *Sabal* species. Orange-colored compounds showed docking scores <-7 kca/mol against 5-α-reductase 2, but got high ΔG binding value (>-7kcal/mol).

Fig.S9. Putative compounds annotated from the methanolic extract of the selected *Sabal* species. Orange-colored compounds showed docking scores <-7 kca/mol against 5-α-reductase 2, but got high ΔG binding value (>-7kcal/mol). Green-colored compounds got docking score and ΔG binding value <-7 kcal/mol.

Fig.S10. Putative compounds annotated from the methanolic extract of the selected *Sabal* species.

Material and Methods (described in detail)

DNA Fingerprinting

SCoT-PCR Amplification

SCoT PCR amplification was carried out according to the procedure described by (Atia, et al. 2017). A set of 15 SCoT primers were tested against the four Sabal species. PCR was carried out in 25 µL reaction mixtures containing 1X PCR buffer, 1.5 mM MgCl2, 0.2 µM of each dNTPs, 1 µM of primer, 1U Go-Taq Flexi polymerase (Promega) and 25 ng genomic DNA.

Thermocycling amplification was performed in a Perkin-Elmer/ Gene Amp PCR system 9700 (PE Applied Biosystem). The amplification was programmed at 94ºC for 5 min as an initial denaturation cycle, followed by 35 cycles, each cycle comprised of (94ºC for 1min, 50ºC for 1min, then 72ºC for 90 s) with a final extension at 72ºC for 7 min. The amplification products were resolved by electrophoresis in a 1.5% agarose gel containing ethidium bromide (0.5ug/mL) in 1X TBE buffer. A 100 bp plus DNA ladder was used as molecular size standards. PCR products were visualized on UV light and photographed using a Gel Doc™ XR+ System with Image Lab™ Software (Bio-Rad®).

CBDP-PCR Amplification

Sixteen CBDP primers (Table S2), used in the current study, were designed according to Singh et al., (2014). PCR was performed in 25 µL reaction total volume containing 1X PCR buffer, 1.5 mM MgCl2, 0.2 µM of each dNTPs, 1 µM of primer, 1U Go-Taq Flexi polymerase (Promega) and 40 ng genomic DNA. Thermocycling amplification was performed in a Gene Amp 9700 PCR system (Applied Biosystem, USA). The PCR amplification was programmed as follows: 94ºC for 5 min as an initial denaturation cycle, followed by 35 cycles, each cycle comprised of (94ºC for 1min, 50ºC for 1min, then 72ºC for 90 s) with a final extension at 72ºC for 7 min. The PCR products were resolved on 1.5% agarose gel containing ethidium bromide (0.5ug/mL) in 1X TBE buffer. A 100 bp plus and 1Kb DNA ladder were used as molecular size

standards. Finally, PCR products were visualized on UV light and photographed using a Gel Doc™ XR+ System with Image Lab™ Software (Bio-Rad®).

Data Analysis

For SCoT and CBDP data analysis, the amplified bands were scored manually. The bands were scored as absent (0) or present (1) to create the binary data matrix. A similarity matrix was constructed according to the Jaccard similarity coefficient (Atia et al., 2021). For SCoT, and CBDP marker systems data, dendrograms were developed using cluster analysis and the unweighted pair group method of arithmetic averages (UPGMA).

Experimental Design

Castration of Male Rats (Orchiectomy).

On the experiment day, rats were anaesthetized with an intraperitoneal injection of ketamine (50 mg/kg) and xylazine (8 mg/kg). Castration of the rats was carried out according to a previously described method (Sandow 2016 Massey et al. 2011; Gray et al. 2005). Briefly, the skin was disinfected with surgical povidone iodine (10%) before a midline incision of 1 cm was made through the skin and the underlying skeletal muscle layer to expose the testes. Prior to bilateral orchiectomy, the vas deferens, testicular artery and veins were ligated by a 4-0 bioabsorbable surgical suture. Finally, the midline incision was sutured using a 3-0 silk surgical suture. Then all animals were given amoxicillin (50 mg/k, i.m.) as prophylaxis against postoperative infections. Sham-operated rats have experienced the same surgical procedure except for the step of orchidectomy and ligation. The experimental work carried out in this study was approved by the Commission on Ethics of Scientific Research, Faculty of Pharmacy, Minia University (Project: ES03/2020)

Cell culture

Human Benign Prostatic Hyperplasia (BPH-1) and human prostatic stromal myofibroblast (WPMY-1) Cell Lines were added for 4–6 h in the incubator maintained at 5% CO2 at 37°C. Detached cells were collected and centrifuged at 1000 RPM for 3 min and transferred to a culture flask and incubated at 37 °C, 5% CO2 in air atmosphere for 24 h. When up to 80% to 90% confluence, the cells were harvested by using 0.25% Trypsin-EDTA (Gibco, Invitrogen). Then, cells were replanted into 10 cm culture plates at the appropriate density and cell morphology and adherence were evaluated. cells were cultured using DMEM (Invitrogen/Life Technologies) supplemented with 10% FBS (Hyclone,), to make the complete growth medium,

10 ug/ml of insulin (Sigma), and 1% penicillin-streptomycin. All of the other chemicals and reagents were from Sigma, or Invitrogen. Plate cells (cells density 1.2 – 1.8 × 10,000 cells/well) in a volume of 100µl complete growth medium + 100 ul of the tested extract per well in a 96-well plate for 24 hours before the MTT assay. All operations should be carried out under strict aseptic conditions. Remove culture medium to a centrifuge tube. Briefly rinse the cell layer with 0.25% (w/v) Trypsin 0.53 mM EDTA solution to remove all traces of serum which contains Trypsin inhibitor. Add 2.0 to 3.0 ml of Trypsin EDTA solution to flask and observe cells under an inverted microscope until cell layer is dispersed (within 5 to 15 minutes). Note: To avoid clumping do not agitate the cells by hitting or shaking the flask while waiting for the cells to detach. Cells that are difficult to detach may be placed at 37°C to facilitate dispersal. Add 6.0 to 8.0 mL of complete growth medium and aspirate cells by gently pipetting. Transfer the cell suspension to the centrifuge tube with the medium and cells and centrifuge at approximately 125 xg for 5 to 10 minutes. Discard the supernatant. Resuspend the cell pellet in fresh growth medium. Add appropriate aliquots of the cell suspension to new culture vessels. Incubate cultures at 37°C for 24 hrs.8-After treatment of cells with the serial concentrations of the selected extracts (63, 125, 250, 500 and 1000 µg/ml) to be tested incubation is carried out for 48 h at 37ºC, then the plates are to be examined under the inverted microscope and proceed for the MTT assay.

MTT – Cytotoxicity assay

Remove cultures from incubator into laminar flow hood or other sterile work area. Reconstitute each vial of MTT [M-5655] to be used with 3 ml of medium or balanced salt solution without phenol red and serum. Add reconstituted MTT in an amount equal to 10% of the culture medium volume. Return cultures to incubator for 2-4 hours depending on cell type and maximum cell density. (An incubation period of 2 hours is generally adequate but may be lengthened for low cell densities or cells with lower metabolic activity.) Incubation times should be consistent when making comparisons. After the incubation period, remove cultures from incubator and dissolve the resulting formazan crystals by adding an amount of MTT Solubilization Solution [M-8910] equal to the original culture medium volume. Gentle mixing in a gyratory shaker will enhance dissolution. Occasionally, especially in dense cultures, trituration may be required to completely dissolve the MTT formazan crystals. Spectrophotometrically measure absorbance at a wavelength of 570 nm. Measure the background absorbance of multi-well plates at 690 nm and subtract from the 450 nm measurement. Tests performed in multi-well plates can be read using the appropriate type of

plate reader or the contents of individual wells may be transferred to appropriate size cuvettes for spectrophotometric measurement.

LC-HRMS metabolomic analysis

Metabolomic profiling of the methanolic fruits extracts of *S. blackburniana, S. causiarum, S. palmetto* and *S. yapa* was performed using an Acquity Ultra Performance Liquid Chromatography system coupled to a Synapt G2 HDMS quadrupole time-of-flight hybrid mass spectrometer (Waters, Milford, USA). The HPLC column, a BEH C18 column (2.1 × 100 mm, 1.7 µm particle size; Waters, Milford, CT, USA) with a guard column (2.1 × 5 mm, 1.7 µm particle size) and a linear solvent gradient of 0–100% eluent B at a flow rate of 300 µL/min over 5 min, using 0.1% formic acid in water (v/v) as solvent A and acetonitrile as solvent B was used for chromatographic separation. The column temperature was 40°C and the injection volume was 2 µL. The total analysis time for each sample was 45 min. The dereplication of each m/z ion peak was achieved, metabolites recorded in the customized databases based on established parameters (m/z threshold of ± 3 ppm and retention time). Conversion of the raw data into sliced positive and negative ionization files was performed via MS-convert software. Negative and positive ionization switch modes were used to include the highest number of metabolites from the investigated plant extracts. The obtained files were subjected to the data mining MZmine 2.10 software (Okinawa Institute of Science and Technology Graduate University, Japan) for deconvolution, peak picking, alignment, deisotoping, and formula prediction.

In silico study

Molecular Docking

AutoDock Vina software was used in all molecular docking experiments (Gong, et al.,2006). ll annotated compounds were docked against the human 5-α-reductase 2 crystal structure (PDB codes: 7BW1) (Seeliger, D and de Groot, B.L. ,2010). The binding site was determined according to the enzyme's co-crystallized ligand. The active site of the enzyme is relatively flexible and, to account for this flexibility, we used MDS-derived conformers sampled every 25 ns for docking experiments (i.e., ensemble docking) (Jin, etal.,2020; Sayed, et al.,2020) Subsequently, we ranked the resulting top hits according to their calculated binding energies. Docking poses were analyzed and visualized using Pymol software (Gong, et al.,2006).

Binding Free Energy Calculations

Binding free energy calculations (ΔG) were performed using the free energy perturbation (FEP) method (Kim, et al., 2020). This method was described in detail in the recent article by Kim and coworkers (Amaro et al.,2018). Briefly, it calculates the binding free energy ΔGbinding according to the following equation: ΔGbinding = ΔGComplex − ΔGLigand. The value of each ΔG is estimated from a separate simulation using NAMD software. Interestingly, all input files required for simulation by NAMD (Bowers, et al.,2006; Kim, et al., 2020), can be papered by using the online website Charmm-GUI (https://charmm-gui.org/?doc=input/afes.abinding, accessed on 18 May 2021. Subsequently, we can use these files in NAMD to produce the required simulations using the FEP calculation function in NAMD. The equilibration was achieved in the NPT ensemble at 300 K and 1 atm (1.01325 bar) with Langevin piston pressure (for" Complex" and" Ligand") in the presence of the TIP3P water model. Then, 10 ns FEP simulations were performed for each compound, and the last 5 ns of the free energy values was measured for the final free energy values (Amaro et al.,2018). Finally, the generated trajectories were visualized and analyzed using VMD software.

Table S1: Primer Name, sequences, number of total bands, polymorphic bands, percentage of polymorphism of SCoT primers.

Primer Name	Sequence	Number of Bands		% of polymorphism
		Total	Polymorphic	
SCoT-1	**CAACAATGGCTACCACCA**	8	5	62.5
SCoT-3	**CAACAATGGCTACCACCG**	10	8	80.0
SCoT-4	**CAACAATGGCTACCACCT**	12	9	75.0
SCoT-5	**CAACAATGGCTACCACGA**	13	7	53.8
SCoT-6	**CAACAATGGCTACCACGC**	12	9	75.0
SCoT-8	**CAACAATGGCTACCACGT**	14	11	78.6
SCoT-9	**CAACAATGGCTACCAGCA**	12	10	83.3
SCoT-10	**CAACAATGGCTACCAGCC**	8	6	75.0
SCoT-11	**AAGCAATGGCTACCACCA**	11	7	63.6
SCoT-12	**ACGACATGGCGACCAACG**	13	8	61.5
SCoT-13	**ACGACATGGCGACCATCG**	14	10	71.4
SCoT-14	**ACGACATGGCGACCACGC**	10	6	60.0
SCoT-15	**ACGACATGGCGACCGCGA**	9	5	55.6
SCoT-24	**CACCATGGCTACCACCAT**	11	7	63.6
SCoT-25	**ACCATGGCTACCACCGGG**	9	6	66.7
Total		166	114	68.7
Average		11.07	7.6	

Table S2: Genetic similarities between the four *Sabal* species based on Jaccard's similarity coefficient of SCoT data.

	S. causiarum	*S. blackburniana*	*S. palmetto*	*S. yapa*
S. causiarum	100%	--	--	--
S. blackburniana	88%	100%	--	--
S. palmetto	82%	80%	100%	--
S. yapa	79%	76%	78%	100%

Table S3: Primer Name, sequences, number of total bands, polymorphic bands, percentage of polymorphism of CBDP primers.

Primer Code	Primer Sequence	Number of Bands		% of polymorphism
		Total	Polymorphic	
CAAT-2	**TGAGCACGATCCAATAAT**	9	6	66.7
CAAT-3	**TGAGCACGATCCAATACC**	11	8	72.7
CAAT-4	**TGAGCACGATCCAATAAG**	13	8	61.5
CAAT-5	**TGAGCACGATCCAATCTA**	14	10	71.4
CAAT-6	**TGAGCACGATCCAATCAG**	13	8	61.5
CAAT-7	**TGAGCACGATCCAATCGA**	15	11	73.3
CAAT-8	**TGAGCACGATCCAATCGG**	16	10	62.5
CAAT-9	**TGAGCACGATCCAATGAT**	11	7	63.6
CAAT-10	**TGAGCACGATCCAATGTT**	11	8	72.7
CAAT-11	**TGAGCACGATCCAATTGC**	12	10	83.3
CAAT-12	**TGAGCACGATCCAATATA**	13	7	53.8
CAAT-14	**TGAGCACGATCCAATGCG**	7	3	42.9
CAAT-15	**TGAGCACGATCCAATTGA**	9	4	44.4
CAAT-16	**TGAGCACGATCCAATTCA**	12	6	50.0
CAAT-17	**TGAGCACGATCCAATTTG**	11	7	63.6
CAAT-19	**CTGAGCACGATCCAATAC**	10	6	60.0
Total		187	119	63.6
Average		11.69		7.44

Table S4: Genetic similarities between the four *Sabal* species based on Jaccard's similarity coefficient of CBDP data.

	S. causiarum	*S. blackburniana*	*S. palmetto*	*S. yapa*
S. causiarum	100%	--	--	--
S. blackburniana	87%	100%	--	--
S. palmetto	83%	81%	100%	--
S. yapa	84%	79%	85%	100%

187 Table.S5. The Reduction% in weights of sex organs of male *Sprague Dawley* rats after administration of the
188 fruit methanolic extracts of *S. blackburniana, S, causiarum* and *S. palmetto*.

Tested groups	Reduction% in weights of sex organs					
	Prostate weight	P W/B W index	Seminal Vesicle weight	SV/B W index	Levator ani weight	L A/B W index
T +*S. blackburniana*	54.10%*	51.50%*	37.75%*	33.64%*	44.33%*	40.06%*
T +*S. causiarum*	52.30% *	55.20%*	32.93%*	35.93%*	21.58%**	26.43%**
T + *S. palmetto*	34.85%*	35.39%*	9.57%	8%	23.05%**	24.62%**

189 Significant from Testosterone group (T) at $p<0.05$ ** Significant from Testosterone group (T) at $p<0.01$. Data was
190 analysed using one-way ANOVA followed by Tukey's post-comparison test.

191 .

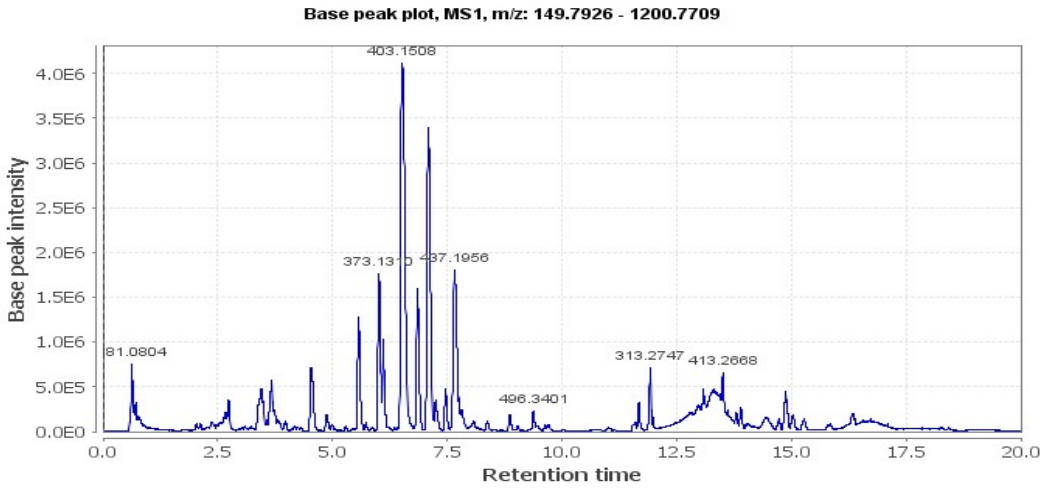

192

193 **Fig (S1):** Total ion chromatogram of *S. blackburniana* fruits (negative ionization mode).

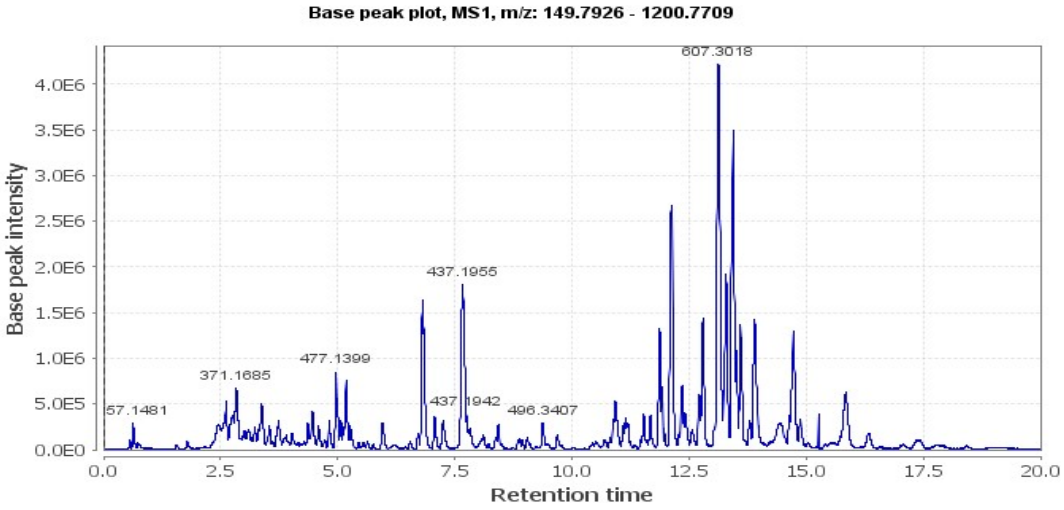

194

195 **Fig (S2):** Total ion chromatogram of *S. yapa* fruits (negative ionization mode).

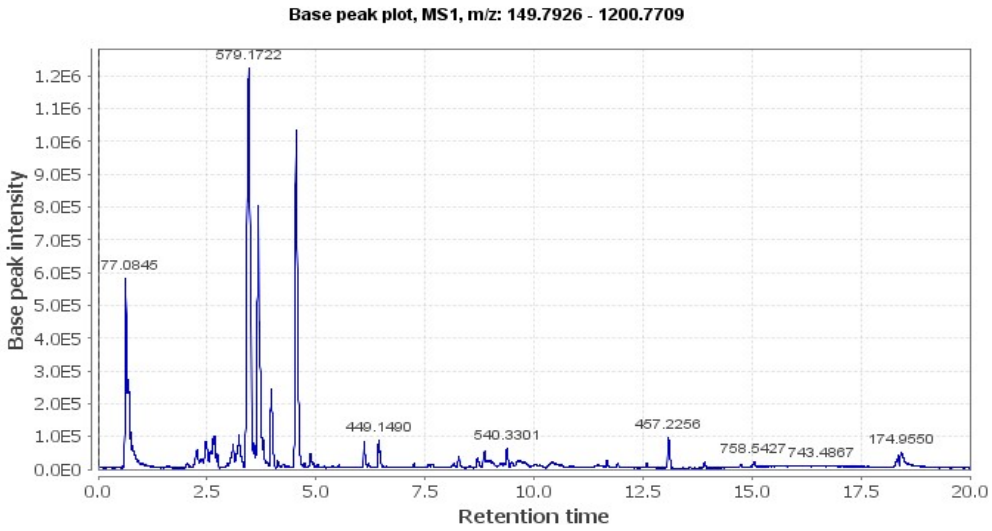

196

197 **Fig (S3):** Total ion chromatogram of *S. palmetto* fruits (negative ionization mode).

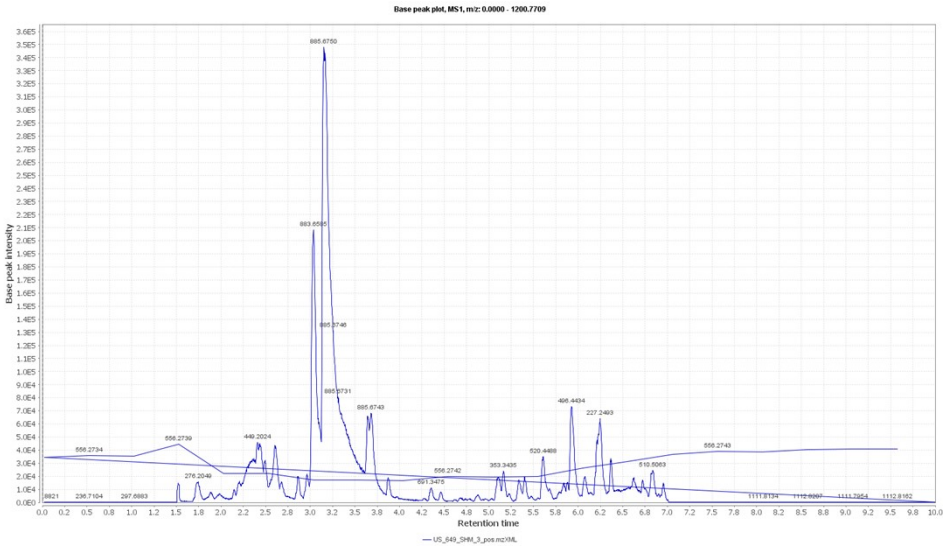

198

199 **Fig (S4): Total ion chromatogram of *S. causiarum* fruits (positive ionization mode)**

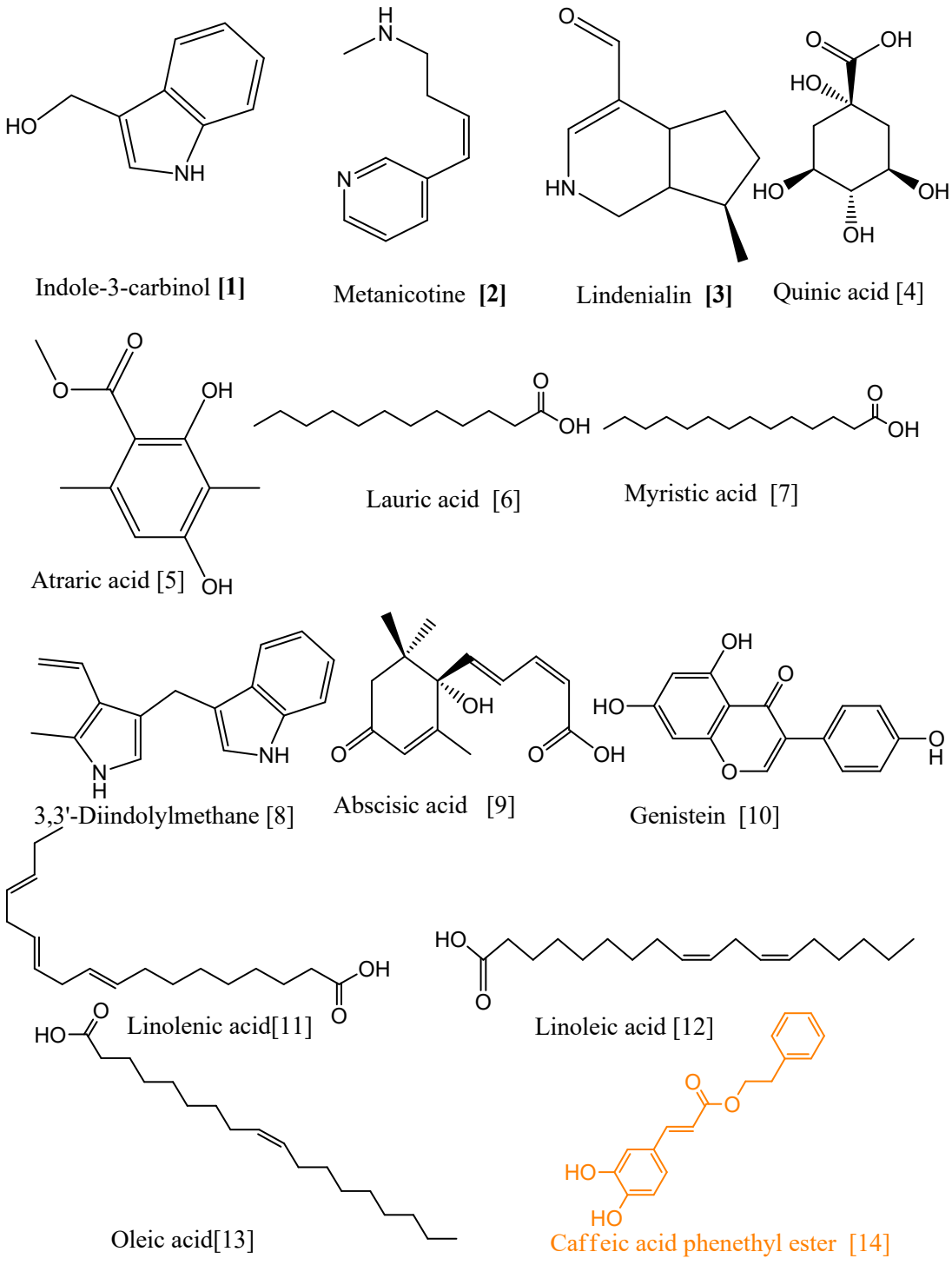

Fig.S5. Putative compounds annotated from the methanolic extract of the selected *Sabal* species. Orange-colored compounds showed docking scores <-7 kca/mol against 5-α-reductase 2, but got high $\Delta G_{binding}$ value (>-7kcal/mol).

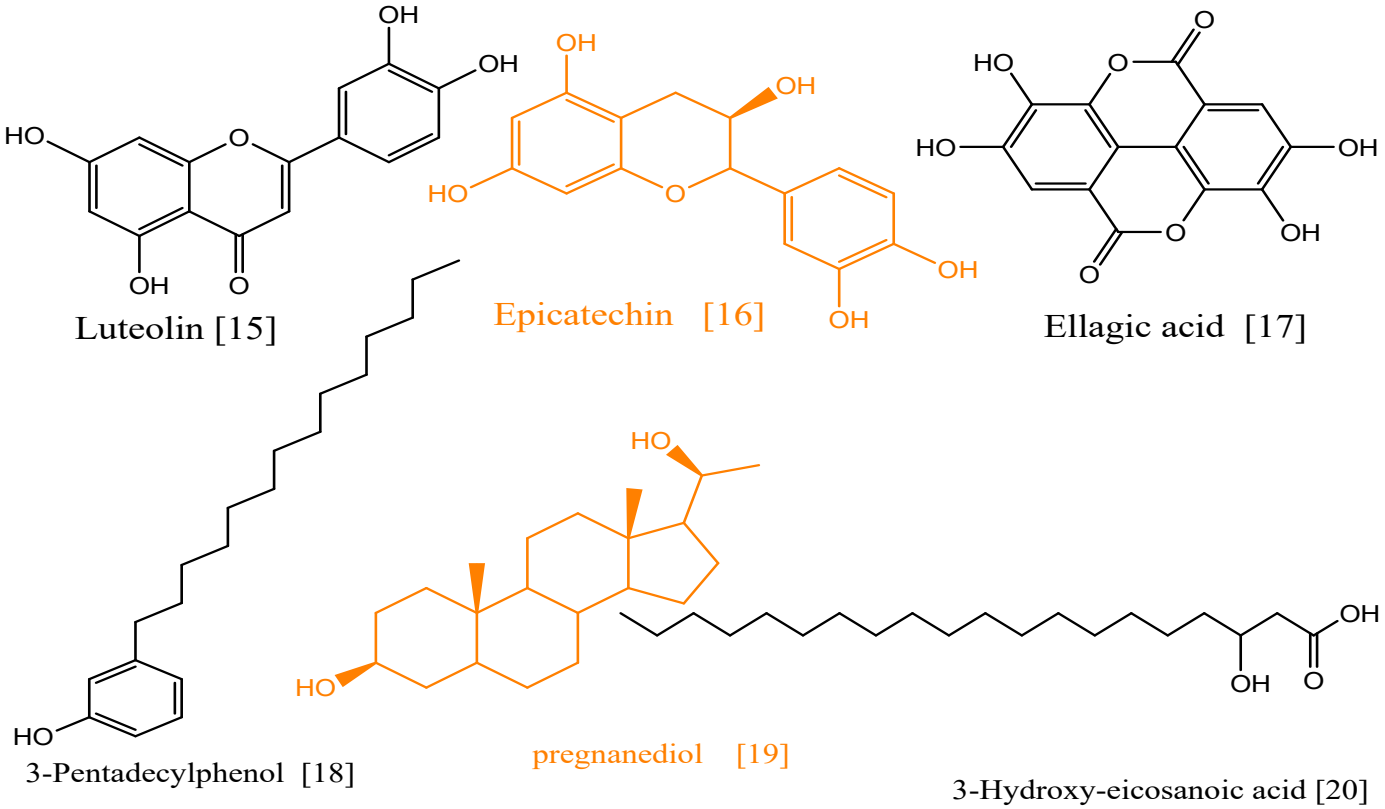

208
209

210

211 **Fig.S6.** Putative compounds annotated from the methanolic extract of the selected *Sabal* species.
212 Orange-colored compounds showed docking scores <-7 kca/mol against 5-α-reductase 2, but got high
213 $\Delta G_{binding}$ value (>-7kcal/mol). Green-colored compounds got docking score and $\Delta G_{binding}$ value <-7
214 kcal/mol.

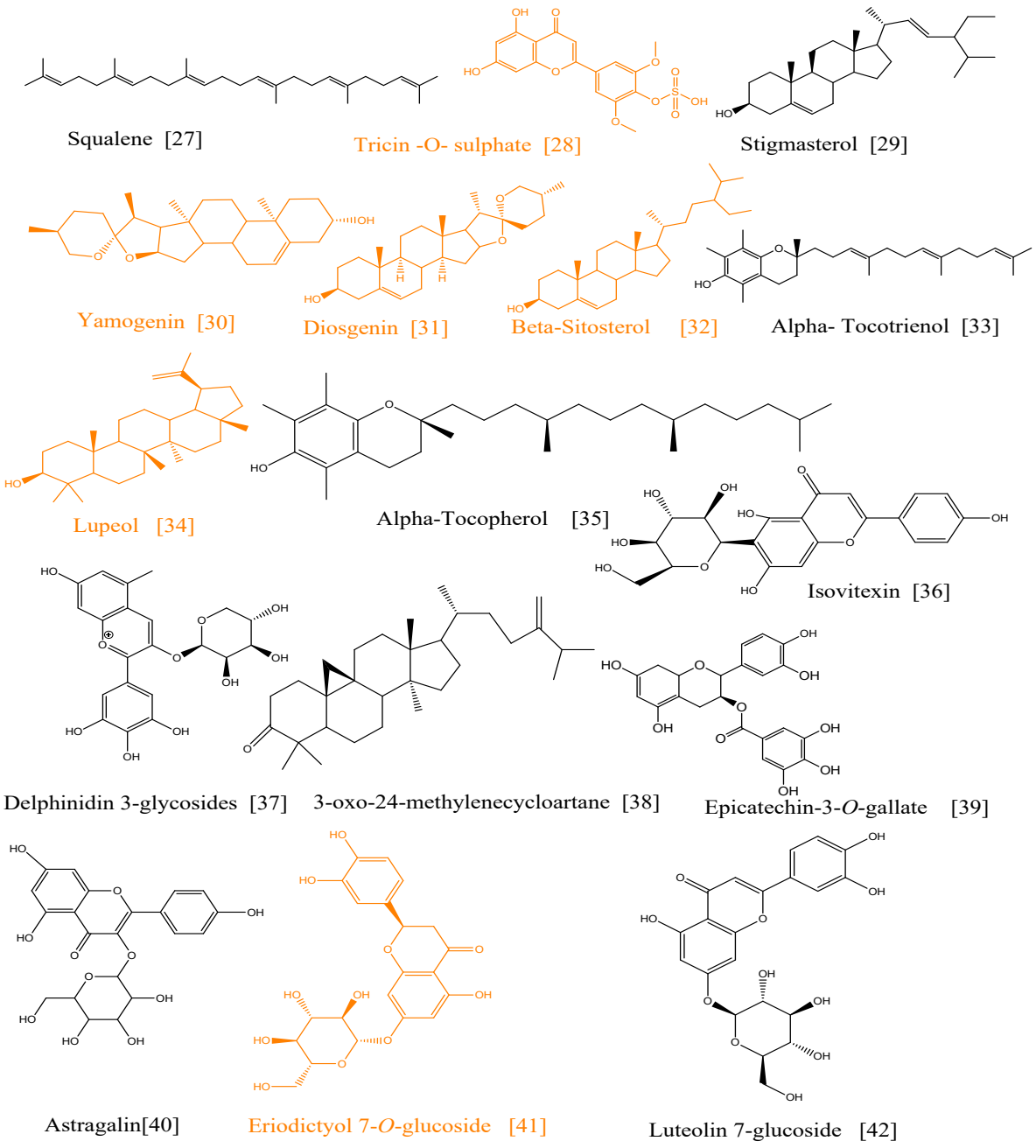

Fig.S7. Putative compounds annotated from the methanolic extract of the selected *Sabal* species. Orange-colored compounds showed docking scores <-7 kca/mol against 5-α-reductase 2, but got high $\Delta G_{binding}$ value (>-7kcal/mol).

224

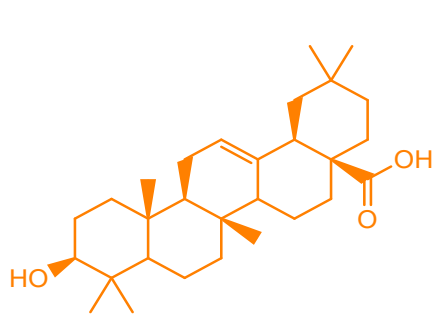

Oleanolic acid[43]

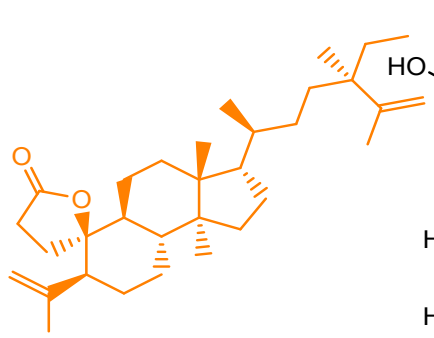

Sablacaurin B[44]

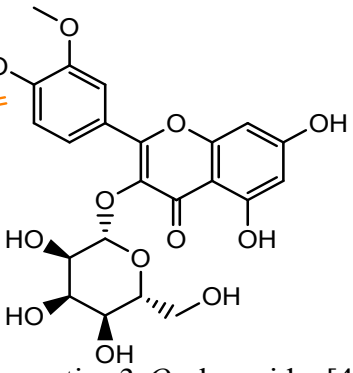

Isorhamnetin -3-*O*-glucoside [45]

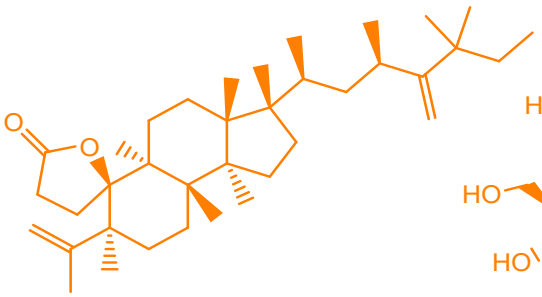

Sablacaurin A[46]

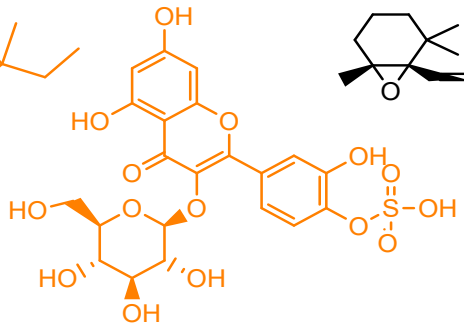

Quercetin-3-O-glucoside sulphate[47]

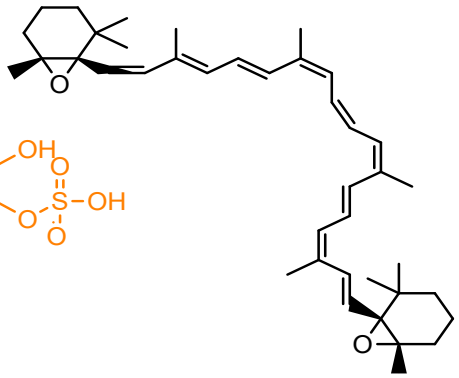

Beta- Carotene diepoxide [48]

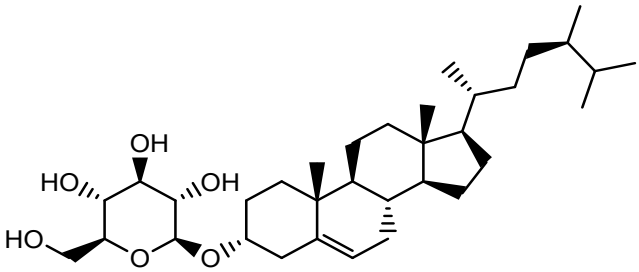

Beta--sitosterol-3-O- Beta--d-glucoside [49]

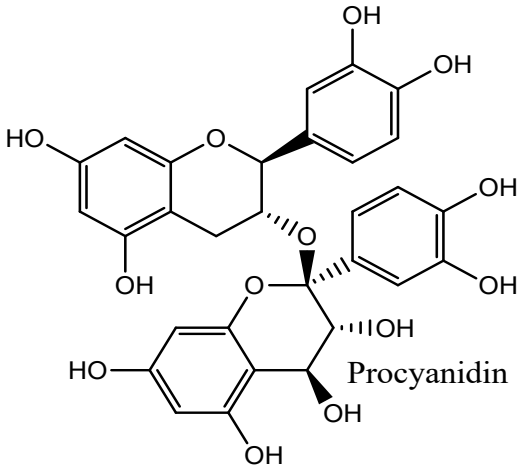

Procyanidin [50]

225
226

227 **Fig.S8.** Putative compounds annotated from the methanolic extract of the selected *Sabal* species.
228 Orange-colored compounds showed docking scores <-7 kca/mol against 5-α-reductase 2, but got high
229 $\Delta G_{binding}$ value (>-7kcal/mol).

230

231

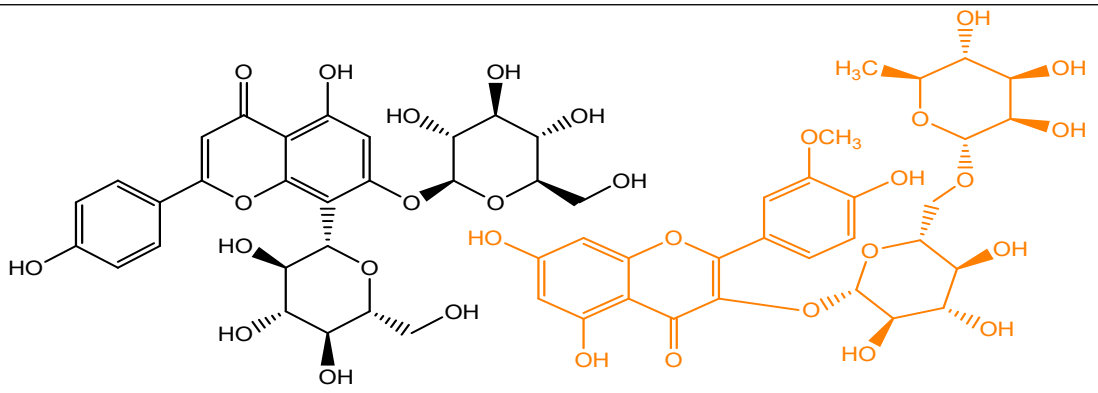

vitexin-7-O-glucoside [51]

Isorhamnetin-3-O-rutinoside[52]

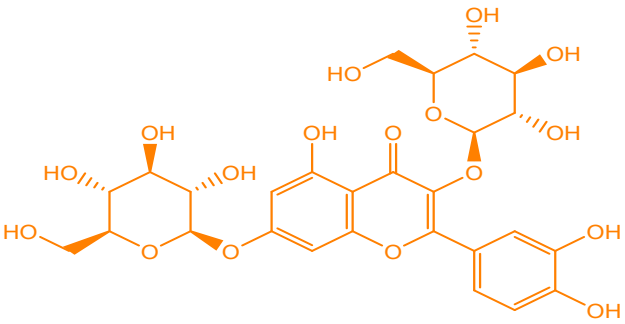

Quercetin 3,7-diglucoside [53]

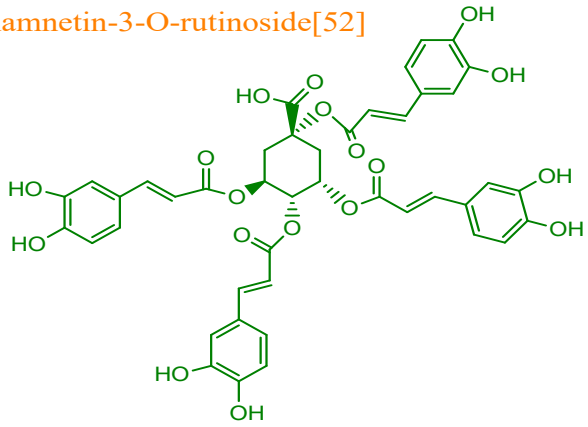

Tetra-*O*-caffeoylquinic acid [54]

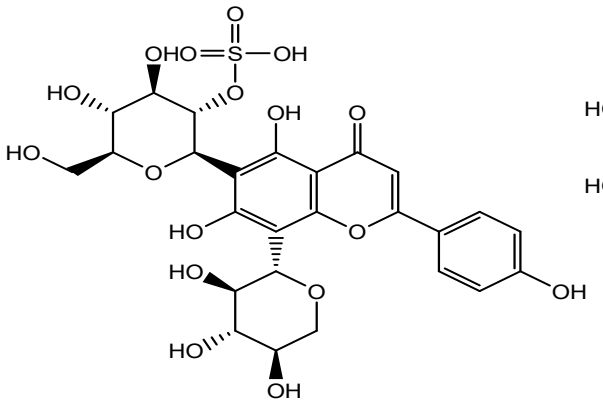

Apigenin-6-glucoside-8-arabinoside sulphate [55]

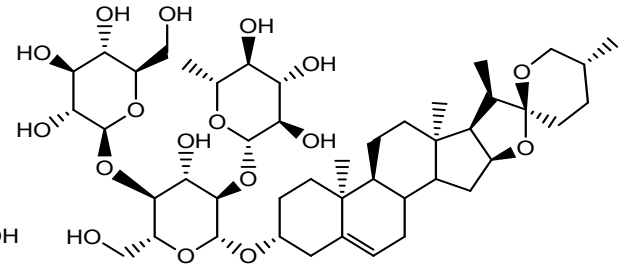

Deltonin [56]

Fig.S9. Putative compounds annotated from the methanolic extract of the selected *Sabal* species. Orange-colored compounds showed docking scores <-7 kca/mol against 5-α-reductase 2, but got high $\Delta G_{binding}$ value (>-7kcal/mol). Green-colored compounds got docking score and $\Delta G_{binding}$ value <-7 kcal/mol.

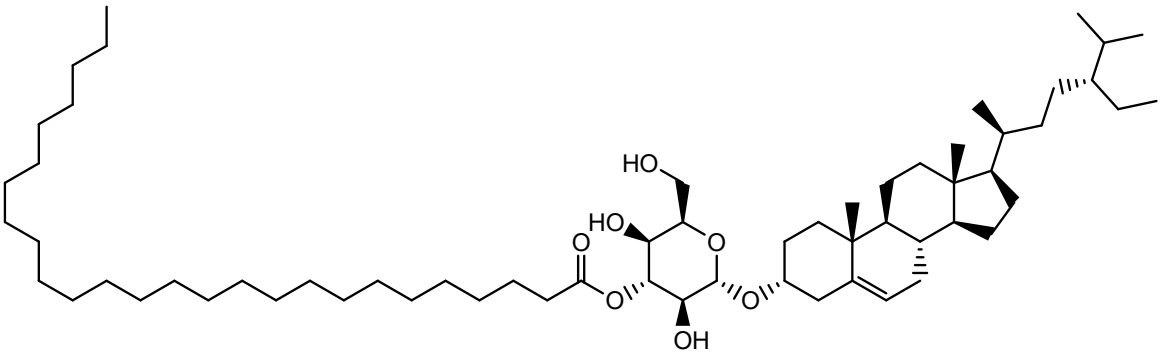

Beta-sitosterol glucoside-3'-O-hexacosanoicate [58]

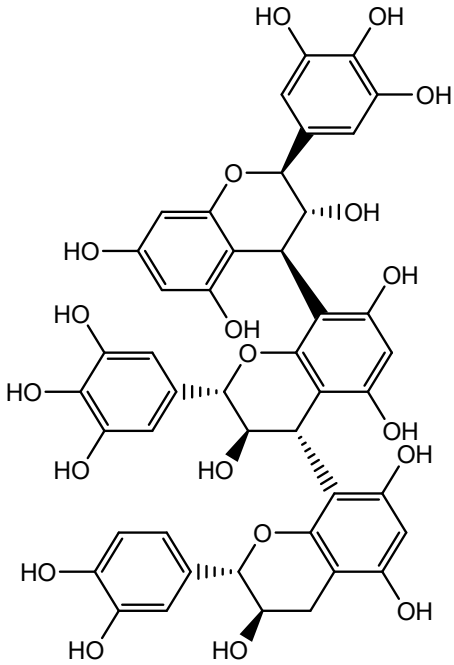

Gallocatechin-(4alpha-8)]2-catechin [57]

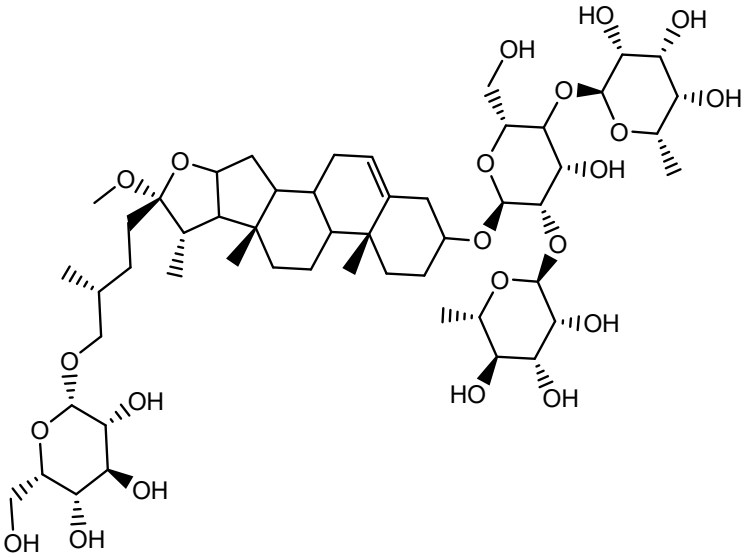

Methylprotodioscin [59]

Fig.S10. Putative compounds annotated from the methanolic extract of the selected *Sabal* species.

References

Atia, M.A., Sakr, M.M. and Adawy, S.S., 2017. Assessing date palm genetic diversity using different molecular markers. In Date Palm Biotechnology Protocols Volume II (pp. 125-142). Humana Press, New York, NY.

Singh AK, Rana MK, Singh S, Kumar S, Kumar R, Singh R. CAAT box-derived polymorphism (CBDP): a novel promoter-targeted molecular marker for plants. *Journal of Plant Biochemistry and Biotechnology*. 2014 Apr 1;23(2):175-83.

Atia M, Abd El-Moneim D., Abdelmoneim T.K., Reda E.H., Abdel Shakour Z. T., El-Halawany A.M, El-Kashoury E. A., Shams K.A., Abdel-Azim N. S & Hegazy M., 2021.Evaluation of genetic variability and relatedness among eight *Centaurea* species through CAAT-box derived polymorphism (CBDP) and start codon targeted polymorphism (SCoT) markers, *Biotechnology & Biotechnological Equipment*, 35:1, 1230-1237.

Gray, L.E Jr., Furr, J and Ostby, J.S., 2005. Hershberger assay to investigate the effects of endocrine disrupting compounds with androgenic and antiandrogenic activity in castrate-immature male rats. *In: Current Protocols in Toxicology* 16.9.1-16.9.15.

Massey C, Dhuyvetter KC, Llewelyn et al. ,2011. Castration and morbidity and their effects on performance, carcass quality, and price differentials for bulls and steers. *The Professional Animal Scientist* 27:19-28

Seeliger, D.; de Groot, B.L. Ligand docking and binding site analysis with PyMOL and Autodock/Vina. *J. Comput. Aided Mol. Des*. 2010, 24, 417–422.

Jin, Z.; Du, X.; Xu, Y.; Deng, Y.; Liu, M.; Zhao, Y.; Zhang, B.; Li, X.; Zhang, L.; Peng, C.; et al. Structure of M pro from SARS-CoV-2 and discovery of its inhibitors. *Nature* 2020, 582, 289–293.

Sayed, A.M.; Alhadrami, H.A.; El-Gendy, A.O.; Shamikh, Y.I.; Belbahri, L.; Hassan, H.M.; Abdelmohsen, U.R.; Rateb, M.E. Microbial natural products as potential inhibitors of SARS-CoV-2 main protease (Mpro). *Microorganisms* 2020, 8, 970

Amaro, R.E.; Baudry, J.; Chodera, J.; Demir, Ö.; McCammon, J.A.; Miao, Y.; Smith, J.C. Ensemble docking in drug discovery. *Biophys. J.* 2018, 114, 2271–2278.

Kim, S.; Oshima, H.; Zhang, H.; Kern, N.R.; Re, S.; Lee, J.; Rous, B.; Sugita, Y.; Jiang, W.; Im, W. CHARMM-GUI free energy calculator for absolute and relative ligand solvation and binding free energy simulations. *J. Chem. Theory Comput*. 2020, 16, 7207–7218.

Bowers, K.J.; Chow, D.E.; Xu, H.; Dror, R.O.; Eastwood, M.P.; Gregersen, B.A.; Klepeis, J.L.; Kolossvary, I.; Moraes, M.A.; Sacerdoti, F.D.; et al. Scalable algorithms for molecular dynamics simulations on commodity clusters. In Proceedings of the SC'06: Proceedings of

the 2006 ACM/IEEE Conference on Supercomputing, Tampa, FL, USA, 11–17 November 2006; *IEEE: New York, NY, USA*, 2006; p. 43.

Phillips, J.C.; Braun, R.; Wang, W.; Gumbart, J.; Tajkhorshid, E.; Villa, E.; Chipot, C.; Skeel, R.D.; Kalé, L.; Schulten, K. Scalable molecular dynamics with NAMD. *J. Comput. Chem.* 2005, 26, 1781–1802.

El-Hawwary, S. S. Abd Almaksoud, H. M. Saber, F. R. Elimam, H. Sayed A.M, M.A. El Raey, Abdelmohsen. U R., 2021. Green Synthesized Zinc Oxide Nanoparticles, Anti-Alzheimer Potential and Metabolic Profiling of *Sabal blackburniana* grown in Egypt supported by molecular modelling, *RSC Adv.*11,18009.

El-Hawwary, S. S. Saber, F. R, Abd Almaksoud, H. M. Elimam, H. Sayed A.M, Abdelmohsen. U R. Cytotoxic potential of three *Sabal* species grown in Egypt: a metabolomic and docking-based study. *Nat. Prod. Res*., 19 (2020), pp. 1-6

A. Fahmi., M.A. El Raey., A. Y. Ibrahim., M.A.O. Abdelfattah. A. M. Abdelmageed., M. Sobeh., 2021.A sulfated polyphenols-rich extract from *Sabal yapa* exhibits antitumor ractivities in Ehrlich ascites carcinoma. *Saudi Journal of Biological Sciences*, 28(5), 3117-3125.

D.Roell., A. Baniahmad., 2011.The natural compounds atraric acid and N-butyl benzene-sulfonamide as antagonists of the human androgen receptor and inhibitors of prostate cancer cell growth. *Molecular and Cellular Endocrinology*, 332, 1–2, 1-8.

Ammar, N.M., Hefnawy.M. S. Mohamed, D., Agoor, F., 2013. Antiandrogenic and phytochemical evaluation of solvents and supercritical CO2 extracts of *Sabal yapa* fruit cultivated in Egypt. *Rivista Italiana delle Sostanze Grasse*; 90 (4), 229-235.

Hänsel, R. ,1991. Phytopharmaka. 2nd ed. Springer Berlin-Heidelberg-New York.

Gong Y, Firestone G.L, Bjeldanes L.F. 3,3′-Diindolylmethane is a novel topoisomerase IIα catalytic inhibitor that induces S-phase retardation and mitotic delay in human hepatoma HepG2 cells. *Molecular Pharmacology*. 69(4) (2006)1320–1327

Liu, L., Xiong, C., Zhu, Y., Zhou, H., and Ma, S. 2015. The separation and anticancer activity of active monomers from sabal palm seeds. Beijing Huagong Daxue Xuebao (Ziran Kexueban)/Journal of Beijing University of Chemical Technology (Natural Science Edition), 42 (6), pp. 78-83.

Y J Hong, F. A. Tomas-Barberan, A.A., Kader, AE. Mitchell. The Flavonoid Glycosides and Procyanidin Composition of Deglet Noor Dates (Phoenix dactylifera) *J. Agric. Food Chem. 2006*, 54, 6, 2405–2411.

M. Sobeh, S.A. Hassan, M.A. El Raey, W.A. Khalil, M.A. Hassan, M. Wink Polyphenolics from Albizia harveyi exhibit antioxidant activities and counteract oxidative damage and ultra-structural changes of cryopreserved bull semen *Molecules*, 2017 (1993), p. 22

P. Mämmeläa, H. Savolainen., L. Lindroos., J. Kangas., T. Vartiainene., 2000.Analysis of oak tannins by liquid chromatography-electrospray ionisation mass spectrometry. *Journal of Chromatography A*, 891, 75-83.

Uhlig, S., Negård, M., Heldal, K.K., et al. 2016., Profiling of 3-hydroxy fatty acids as environmental markers of endotoxin using liquid chromatography coupled to tandem mass spectrometry. *J. Chromatogr*. A 1434, 119-236.

Nakano, H., S. Kosemurab, M. Yoshida, T. Suzuki, R. Iwaura, R. Kaji, M. Sakai and K. Hirose.,2010a. Oryzamutaic acids B–G, new alkaloids from an Oryza sativa mutant with yellow endosperm. *Tetrahedron Lett.* 51: 49–53.

Farag, M A. Mohsen, M., Heinke, R., Wessjohann, L. A., 2014. Metabolomic fingerprints of 21 date palm fruit varieties from Egypt using UPLC/PDA/ESI–qTOF-MS and GC–MS analyzed by chemometrics. *Food Research International*;64: 218-226.

El-Dib R., Kaloga, M., Mahmoud I., Soliman H., Moharram F., and Kolodziej H., 2004. Sablacaurin A and B, Two 19-nor3,4-seco-lanostane-type Triterpenoids from *Sabal causiarum* and *Sabal blackburniana*, Respectivrly". *Phytochemistry*, 65: 1153-1157.

Gaceb-Terrak, R., Rahmania, F., 2012.Identification and detection of steroidal saponins of spirostane type in the date palm Phoenix dactylifera L.(Arecaceae). *Acta Botanica Gallica* ,159,4,.477-483.

Yang, X.-H., Cai, Z.-Y., Cai, X., Xu, X.-J., Li, H.-J and Qin, Y, Quality standard of Sabal fruit extract soft capsules. Chinese *Journal of New Drugs*. 24 (24) (2015)2854-2864.

Sen CK, Khanna S, Roy S. Tocotrienols: vitamin E beyond tocopherols. Life Sci. 2006 in press.

Harborne, C. A. Williams, J. Greenham, and P. Moyna. Distribution of charged flavones and caffey1shikimic acid in Palmae. *Phytochemistry* .13(1974)1557-1559.

Liu, G.-L.; Guo, H.-H.; Sun, Y.-M. Optimization of the extraction of anthocyanins from the fruit skin of *Rhodomyrtus tomentosa* (Ait.) Hassk and identification of anthocyanins in the extract using high-performance liquid chromatography-electrospray ionization-mass spectrometry (HPLC-ESI-MS). *Int. J. Mol. Sci*. 2012, 13, 6292–6302.

Idaka, K., Hirai, Y., Shoji, J., 1991. Studies on the constituents of Palmae plants.

V. Steroid saponins and flavonoids of leaves of *Phoenix rupicola*, T. *Anderson, P. loureirii Kunth, P. reclinate NJ Jacquin,* and *Areca strum remanzoffianum* Beccari.

Chem. Pharm. Bull. 39, 1455–1461.

J. Pollier. A. Goossens., 2012, Oleanolic acid. *Phytochemistry*, 77, 10-15.

R. A Hiipakka., H-Z. Zhang, W. D Qing Dai, S. Liao., 2002.Structure-activity relationships for inhibition of human 5alpha-reductases by polyphenols. *Biochem Pharmacol,* 15;63(6):1165-76.

S. Ouafi, R. Gaceb-Terrak, N. Bounaga, P. Lebreton, Compt. rend. *Acad. Sci. Paris*, 1988, III306: 399–404

Tomas Lorente, F. and Ferreres, F. (1988). Sulfatos de flavonoides en frutos ´ de phoenix dactilifera (Flavonoid sulphates from *Phoenix dactylifera* fruits). *Revista de Agroqu´ımica y Tecnolog´ıa de Alimentos*. 28(4): 581–585.

Goupy, P., Hugues, M., Boivin, P., M. Josèphe, M., 1999. Antioxidant composition and activity of barley (*Hordeum vulgare*) and malt extracts and of isolated phenolic compounds. Amiot, *JSFA* ;79, 12,1625-1634.

W.Y. Jin., B. Min, J. Pill Lee, P T. Thuong, H. Lee, K. Song, Y. H. Seong, K. Hwan Bae.,2007. Isolation of constituents and anti-complement activity from *Acer okamotoanum*. *Arch Pharm Res*. 30(2):172-176.

Hifnawy, M.S., Mahrous, A.M., Ashour, R.M., 2016. Phytochemical investigation of *Phoenix canariensis* Hort. ex Chabaud leaves and pollen grains. J. *Appl. Pharm. Sci*. 6, 103–109.